

NRC Publications Archive Archives des publications du CNRC

Variable-strength nonlocal measurements reveal quantum violations of classical counting principles

Lupu-Gladstein, Noah; Pang, Ou Teen Arthur; Ferretti, Hugo; Tham, Weng-Kian; Steinberg, Aephraim M.; Bonsma-Fisher, Kent; Brodutch, Aharon

This publication could be one of several versions: author's original, accepted manuscript or the publisher's version. / La version de cette publication peut être l'une des suivantes : la version prépublication de l'auteur, la version acceptée du manuscrit ou la version de l'éditeur.

For the publisher's version, please access the DOI link below. / Pour consulter la version de l'éditeur, utilisez le lien DOI ci-dessous.

Publisher's version / Version de l'éditeur:

<https://doi.org/10.1073/pnas.2416331122>

Proceedings of the National Academy of Sciences, 122, 7, 2025-02-14

NRC Publications Archive Record / Notice des Archives des publications du CNRC :

<https://nrc-publications.canada.ca/eng/view/object/?id=f7993014-b0db-47cf-a7c3-ae7cd6442126>

<https://publications-cnrc.canada.ca/fra/voir/objet/?id=f7993014-b0db-47cf-a7c3-ae7cd6442126>

Access and use of this website and the material on it are subject to the Terms and Conditions set forth at

<https://nrc-publications.canada.ca/eng/copyright>

READ THESE TERMS AND CONDITIONS CAREFULLY BEFORE USING THIS WEBSITE.

L'accès à ce site Web et l'utilisation de son contenu sont assujettis aux conditions présentées dans le site

<https://publications-cnrc.canada.ca/fra/droits>

LISEZ CES CONDITIONS ATTENTIVEMENT AVANT D'UTILISER CE SITE WEB.


Questions? Contact the NRC Publications Archive team at

PublicationsArchive-ArchivesPublications@nrc-cnrc.gc.ca. If you wish to email the authors directly, please see the first page of the publication for their contact information.

Vous avez des questions? Nous pouvons vous aider. Pour communiquer directement avec un auteur, consultez la première page de la revue dans laquelle son article a été publié afin de trouver ses coordonnées. Si vous n'arrivez pas à les repérer, communiquez avec nous à PublicationsArchive-ArchivesPublications@nrc-cnrc.gc.ca.



Variable-strength nonlocal measurements reveal quantum violations of classical counting principles

Noah Lupu-Gladstein^{a,1} , Ou Teen Arthur Pang^a, Hugo Ferretti^a, Weng-Kian Tham^a, Aephraim M. Steinberg^{a,b}, Kent Bonsma-Fisher^{a,c}, and Aharon Brodutch^a

Affiliations are included on p. 7.

Edited by Yakir Aharonov, Chapman University, Orange, CA; received August 13, 2024; accepted January 3, 2025

We implement a variant of the quantum pigeonhole paradox thought experiment to study whether classical counting principles survive in the quantum domain. We observe strong measurements significantly violate the pigeonhole principle (that among three pigeons in two holes, at least one pair must be in the same hole) and the sum rule (that the number of pigeon pairs in the same hole is the sum of the number of pairs across each of the holes) in an ensemble that is pre- and postselected into particular separable states. To investigate whether measurement disturbance is a viable explanation for these counterintuitive phenomena, we employ a we employ variable-strength nonlocal measurements. As we decrease the measurement strength, we find the violation of the sum rule decreases, yet the pigeonhole principle remains violated. In the weak limit, the sum rule is restored due to the cancellation between two weak values with equal and opposite imaginary parts. We observe the same kind of cancellation at higher measurement strengths, thus raising the question: do strong measurements have imaginary parts?

single photons | quantum paradox | weak measurement

The correspondence between quantum measurements and physical reality has been a source of intense debates since the early days of quantum theory (1–5). One point of contention involves the connection between mathematically defined observables and our classical intuition about what these observables represent. The problem manifests starkly in pre- and postselection (PPS) experiments where a system is first prepared in some initial state $|\psi_i\rangle$ (the preselection), then measured at some intermediate time, then projected onto some final state $|\psi_f\rangle$ (the postselection). Naively interpreting the result of the intermediate measurement as reflecting elements of physical reality can lead to paradoxes (6–19). One resolution invokes measurement back-action, arguing that disturbing measurements do not reveal the properties of a system before it was measured.

We present an experiment that probes the role of back-action in these paradoxes by varying the type and strength of measurement disturbance. The experiment is inspired by the so-called quantum pigeonhole paradox (17, 20). The paradox arises from a counterintuitive prediction that three pigeons placed among two holes can each occupy a different hole. This apparent logical contradiction has been observed indirectly at the weak limit in the correlations of a neutron interferometer (21) and directly at the strong limit, using the Hong–Ou–Mandel effect to check whether a pair of photons are in the same polarization state (22). The results of these experiments, considered individually, have been interpreted without resorting to paradox via local interference and measurement disturbance respectively (19, 23–25). Our experiment investigates the pigeonhole paradox across the full spectrum of measurement strengths. Variable-strength nonlocal measurements rule out local interference as a viable explanation and empirically quantify the role of disturbance.

In our experiment, the “pigeons” are photons in displaced Sagnac interferometers and the “pigeonholes” are the two possible travel directions: clockwise $|\mathcal{C}\rangle$ and anticlockwise $|\mathcal{A}\rangle$ (Fig. 1). The corresponding, observables for a particular pigeon $k \in \{(1, 2, 3)\}$ are the projectors $\Pi_{\mathcal{C}}^k = |\mathcal{C}\rangle^k \langle \mathcal{C}|^k$ and $\Pi_{\mathcal{A}}^k = |\mathcal{A}\rangle^k \langle \mathcal{A}|^k$. Each photon is preselected in the state $|+\rangle^k = (|\mathcal{C}\rangle^k + |\mathcal{A}\rangle^k)/\sqrt{2}$ as it enters the interferometer and later postselected in the state $|+\rangle^k = (|\mathcal{C}\rangle^k + i|\mathcal{A}\rangle^k)/\sqrt{2}$ as it leaves. The quantum pigeonhole paradox concerns the observables $\Pi_{\mathcal{S}}^{k,\ell} = \Pi_{\mathcal{A}}^k \Pi_{\mathcal{A}}^\ell + \Pi_{\mathcal{C}}^k \Pi_{\mathcal{C}}^\ell$, which ask whether a particular pair of photons $(k, \ell) \in \{(1, 2), (1, 3), (2, 3)\}$ traveled the same direction. These observables seem to defy two fundamental counting principles.

Significance

Quantum theory has proven wildly successful in predicting properties of systems whose past or future are specified. Applying the theory to systems with a definite past and future yields infamously counterintuitive predictions, e.g., three quantum pigeons can apparently occupy two pigeonholes without any pair occupying the same pigeonhole. Are such counterintuitive predictions merely an artifact of measurement disturbance? We answer this question empirically by measuring photonic “pigeons” with a variety of different measurement disturbances by implementing a scheme that achieves variable-strength measurements of nonlocal observables. We find that measurement disturbance can explain some, but not all, of the paradoxical phenomena of pre- and postselected systems, thus revealing the strange logic of quantum systems.

Author contributions: N.L.-G., H.F., A.M.S., and A.B. designed research; N.L.-G., O.T.A.P., H.F., W.-K.T., and K.B.-F. performed research; A.B. contributed new reagents/analytic tools; N.L.-G. analyzed data; and N.L.-G., A.M.S., and A.B. wrote the paper.

The authors declare no competing interest.

This article is a PNAS Direct Submission.

Copyright © 2025 the Author(s). Published by PNAS. This article is distributed under Creative Commons Attribution-NonCommercial-NoDerivatives License 4.0 (CC BY-NC-ND).

¹To whom correspondence may be addressed. Email: nlupugla@uottawa.ca.

Published February 14, 2025.

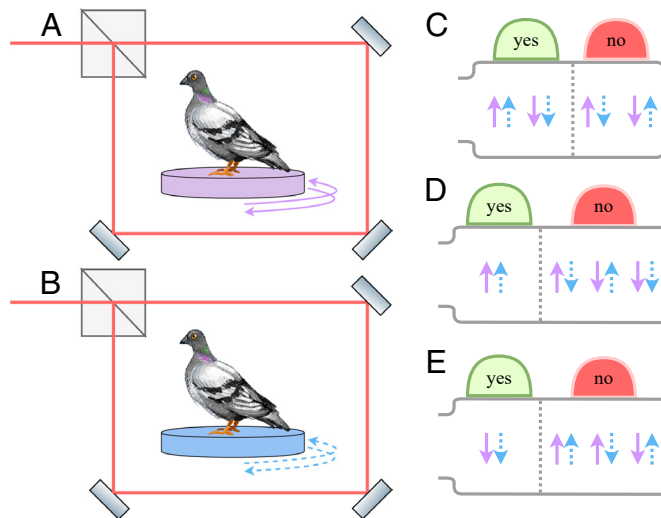


Fig. 1. Conceptual overview. (A and B) Quantum pigeons in two pigeonholes are represented as photons that can propagate clockwise or anticlockwise through a displaced Sagnac interferometer. Beamsplitters prepare the pigeons in $|+\rangle|+\rangle$, then one of the devices (C, D, or E) measures them, then we postselect them onto the state $|+\rangle|+\rangle$ by only detecting photons that exit the same port of the interferometer they entered. (C–E) Different measurements used to observe the pigeons. Panel (C) asks “are both pigeons traveling the same direction?,” panel (D) asks “are both pigeons traveling clockwise?,” and panel (E) asks “are both pigeons traveling anticlockwise?”.

1. The pigeonhole principle: When there are more pigeons than holes, at least one pair must be in the same hole. Violated because $|\langle +i|^k \langle +i|^\ell \Pi_S^{k,\ell} |+\rangle^k |+\rangle^\ell|^2 = 0$.
2. The sum rule: The number of pigeons among two holes is at least the number of pigeons in either hole. Violated because $|\langle +i|^k \langle +i|^\ell \Pi_C^k \Pi_C^\ell |+\rangle^k |+\rangle^\ell|^2 = 1/16 > 0$ and $|\langle +i|^k \langle +i|^\ell \Pi_A^k \Pi_A^\ell |+\rangle^k |+\rangle^\ell|^2 = 1/16 > 0$.

1. The Quantum Pigeonhole Paradox

As a quantum paradox, the pigeonhole paradox exhibits several crucial features. First, the paradox involves correlations in a nonlocal system: each pigeon could be in a different space-like separated region of the galaxy, but quantum mechanics predicts the paradox will occur nevertheless. Second, the preselection and postselection are both separable states, making it difficult to rely on the features of quantum entanglement to explain away the paradox. If entanglement does play a role, it must be generated from the act of observation itself. Finally, these separable states are symmetric, making it irrelevant which particular pair of pigeons are observed.

This last feature is experimentally convenient, as it enables us to measure only a single pair of pigeons. While putting two pigeons in two different holes is trivial, we can still derive a bound that separates intuitive classical behavior from the phenomena arising in the pigeonhole paradox. Suppose three pigeons are placed in two holes according to an arbitrary probability distribution $P(b_1, b_2, b_3)$, where $b_i \in \{C, A\}$ are Boolean variables indicating which of two holes the i th pigeon is placed. Uniformly at random, a pair of pigeons are examined to determine whether or not they are in the same hole. The chance to find the random pair in the same hole is

$$\begin{aligned} & (P(C, C, C) + P(A, A, C) + P(C, C, A) + P(A, A, A) \\ & + P(C, C, C) + P(A, C, A) + P(C, A, C) + P(A, A, A) \\ & + P(C, C, C) + P(C, A, A) + P(A, C, C) + P(A, A, A))/3 \\ & = 1/3 + (P(C, C, C) + P(A, A, A))2/3 \\ & \geq 1/3. \end{aligned}$$

There is no classical distribution of three pigeons across two holes in which a random pair of pigeons is found in the same hole less than 1/3 of the time. In this sense, a measurement of $\Pi_S^{k,\ell}$ that comes out “yes” with any frequency less than 1/3 violates the classical pigeonhole principle. For the rest of the manuscript, we will deal only with Pigeons 1 and 2 without loss of generality, so we set $\Pi_S = \Pi_S^{1,2}$, $\Pi_{CC} = \Pi_C^1 \Pi_C^2$, and $\Pi_{AA} = \Pi_A^1 \Pi_A^2$.

Our experiment hones in on the distinction between an observable and the variety of ways to measure that observable. We compare several different ways to measure Π_S . The first has only two outcomes: {“same direction,” “different direction”}. That is, the measurement reveals whether photons 1 and 2 traveled the same direction, but not which direction they traveled. The second sums the results of {“both clockwise,” “neither clockwise”} and {“both anticlockwise,” “neither anticlockwise”}.

Every yes or “no” question in quantum mechanics can be represented by some projector Π . We will call a measurement of Π “direct” if it indicates whether or not the system was in a yes (or no) state, but not which among potentially many yes (or no) states the system was in. Mathematically, we represent the interaction that generates a direct measurement by a unitary $U_\Pi(s)$ that acts on any system state $|\psi\rangle$ and a particular meter state $|\mu\rangle$ according to

$$U_\Pi(s)|\psi\rangle|\mu\rangle = \Pi|\psi\rangle|s\rangle + (\mathbb{1} - \Pi)|\psi\rangle|-s\rangle, \quad [1]$$

where

$$s = \sqrt{1 - |\langle s | -s \rangle|^2} \quad [2]$$

is the “strength” of the measurement. A strong measurement has $s = 1$, so the yes meter state $|s = 1\rangle$ is orthogonal to the no meter state $|s = -1\rangle$. A weak measurement has $s \ll 1$, meaning the yes and no meter states are nearly indistinguishable. A variable-strength measurement features a strength that can be tuned between these two extremes (16, 26–32).

A single weak measurement provides vanishing information about whether the system was in a yes or no state, but averaging the results of weak measurements across many independent and identical systems yields a meaningful aggregate, the so-called “weak value” (33). The weak value of an observable Π prepared

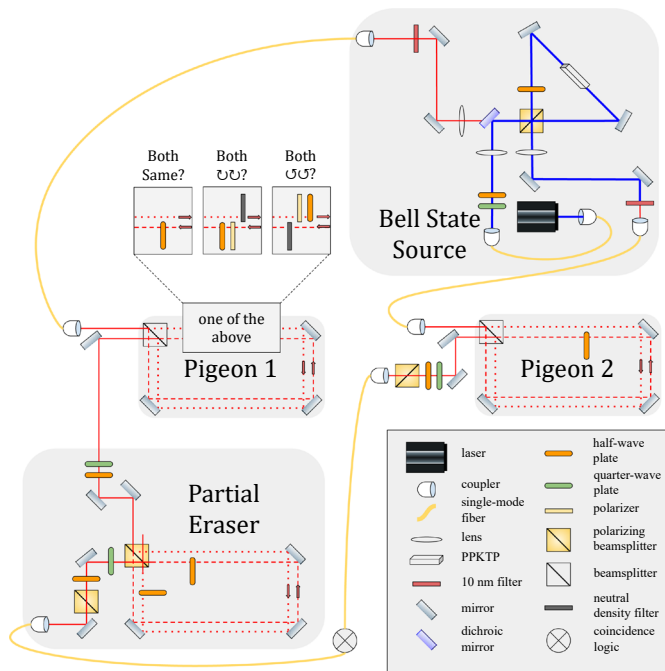


Fig. 2. Experimental setup. A Bell-state source generates polarization-entangled photons by pumping a PPKTP crystal with a continuous-wave laser at 405 nm. Each photon enters a nonpolarizing displaced Sagnac interferometer which allows the photonic pigeon to travel in a superposition of two pigeonholes. The photons are postselected by ignoring an output port of each interferometer. A half waveplate in the anticlockwise path of the Pigeon 2 interferometer performs a strong which-path measurement. The photon is detected and the result of its which-path measurement steers Pigeon 1. One of three different sets of optics in Pigeon 1 encode a strong, direct measurement of either Π_S , Π_{CC} , or Π_{AA} onto polarization. The partial eraser, a displaced Sagnac interferometer, couples polarization to path, and then erases the polarization information. The strength of the polarization-path coupling is set by the angle of two half waveplates inside the partial eraser.

in state $|\psi_i\rangle$ and postselected in state $|\psi_f\rangle$ is the complex number

$$\frac{\langle\psi_f|\Pi|\psi_i\rangle}{\langle\psi_f|\psi_i\rangle}. \quad [3]$$

The real part of the weak value is obtained by measuring the meter in the “real” basis $|\pm \text{Re}\rangle = |s = \pm 1\rangle$. The imaginary part comes from measuring the meter in the “imaginary” basis $|\pm \text{Im}\rangle = (|+\text{Re}\rangle \pm i|-\text{Re}\rangle)/\sqrt{2}$.

In the strong limit, measuring the meter in the real basis gives the probability for the system to have been in a yes state, given the postselection succeeded. This probability is predicted by the Aharonov–Bergmann–Lebowitz formula (34).

$$\frac{|\langle\psi_f|\Pi|\psi_i\rangle|^2}{|\langle\psi_f|\Pi|\psi_i\rangle|^2 + |\langle\psi_f|(1 - \Pi)|\psi_i\rangle|^2}. \quad [4]$$

Curiously, the literature on PPS experiments has so far ignored the strong limit of measuring the meter in the imaginary basis. Even the recent work of De Zela, which studied the role of weak values in strong measurements, did not comment on such strong imaginary measurements (35). The imaginary part of weak values can be related to the sensitivity of the postselection probability to the measurement’s back-action (36). This interpretation holds for strong measurements as well (see Section 4.2 for more details). At all measurement strengths, imaginary parts arise from imaginarity, which has recently been identified as a

useful quantum resource (37–39). The usual model of quantum measurement uses a Gaussian probe, and in fact, this model predicts the imaginary part goes to 0 in the infinitely strong limit (36). However, the decay of the imaginary part to 0 is not a universal feature of quantum measurement. The imaginary part is sensitive to the particular form of the probe (40). For a strong, direct measurement of a projector via a qubit probe, the quantity comes out to

$$\frac{\text{Im}[\langle\psi_i|\psi_f\rangle\langle\psi_f|\Pi|\psi_i\rangle]}{|\langle\psi_f|\Pi|\psi_i\rangle|^2 + |\langle\psi_f|(1 - \Pi)|\psi_i\rangle|^2}. \quad [5]$$

This value is not always 0, which complicates criticisms of the weak value on the basis of its imaginary component (41–43). Strong measurements, at least in some sense, have imaginary parts too.

2. Direct Nonlocal Measurements

Our experiment implements three direct measurements at a continuum of measurement strengths: $U_{\Pi_S}(s)$, $U_{\Pi_{CC}}(s)$, and $U_{\Pi_{AA}}(s)$. These measurements are made on pairs of particles, and must be nondestructive (44). These types of nonlocal measurements are currently attracting considerable attention with a number of recent theoretical proposals (11, 45–51) and experimental results at both the strong limit (52–54) and the weak limit (9, 12, 55). The Hamiltonians that generates variable-strength, direct measurements of two-body observables such as Π_{CC} require three-body interaction terms of the form

$$M^0\Pi^1\Pi^2, \quad [6]$$

where M^0 is some meter observable. Physically, these terms represent a single meter interacting simultaneously with two spatially separate systems. This interaction would have to be nonlocal, and thus unphysical. Nevertheless, it is possible to simulate these interactions using a combination of quantum steering and quantum erasure (45).

The first step in generating these nonlocal interactions is to prepare our photonic pigeons with a shared and entangled polarization probe. We use the Bell state source, illustrated in Fig. 2 and described in detail in Section 4.3 to generate pairs of photons whose joint polarization state is $\frac{|H\rangle|H\rangle + |V\rangle|V\rangle}{\sqrt{2}}$. We use the standard notation $|H\rangle$, $|V\rangle$ for horizontal and vertical polarization respectively and $|D\rangle = (|H\rangle + |V\rangle)/\sqrt{2}$, $|A\rangle = (|H\rangle - |V\rangle)/\sqrt{2}$ for diagonal and antidiagonal respectively. Each photon is then sent into its own displaced Sagnac interferometer, which is opened and closed with a 50/50 beamsplitter to create the initial and final states. The initial state is always $|\psi_i\rangle = |+\rangle|+\rangle$ and the final state, which is selected by only detecting photons that exit the interferometer through the same port they entered and optionally blocking one of the paths is $|\psi_f\rangle \in \{|+\rangle|+\rangle, |C\rangle|C\rangle, |C\rangle|A\rangle, |A\rangle|C\rangle, |A\rangle|A\rangle\}$.

Polarization optics in the Sagnac interferometers perform strong, but nondestructive which-path measurements. The Pigeon 2 interferometer has a half waveplate in its anticlockwise path, but not its clockwise path. Projecting photon 2 onto $|D\rangle$ (which succeeds with probability 1/2) steers Photon 1’s initial polarization to $|D\rangle$ if photon 2 went clockwise and $|A\rangle$ if photon 2 went anticlockwise. At this stage, the polarization-path state (with normalization indicating success probability) is

$$(|D\rangle^1 \otimes \Pi_C^2|\psi_i\rangle^{12} + |A\rangle^1 \otimes \Pi_A^2|\psi_i\rangle^{12})/\sqrt{2}. \quad [7]$$

One of three different strong which-path measurements (shown in Fig. 2), corresponding to Π_S , Π_{CC} , and Π_{AA} , shifts the polarization of photon 1. To measure Π_S , we place a half waveplate in the anticlockwise path, but not in the clockwise path, which evolves the state to

$$(|D\rangle^1 \otimes \Pi_S^{12} |\psi_i\rangle^{12} + |A\rangle^1 \otimes (\mathbb{1} - \Pi_S^{12}) |\psi_i\rangle^{12}) / \sqrt{2}. \quad [8]$$

The polarization of photon 1 at this stage strongly encodes whether both photons have traveled the same direction, but not which direction they traveled.

To measure Π_{CC} , we place a polarizer followed by a half waveplate in the anticlockwise path that together apply the operator $-|A\rangle\langle V|$. Photon 1 only survives this operator with probability 1/2. To keep the interferometer balanced, we place a neutral density filter with transmission probability 1/2 in the clockwise path. The state at this point is

$$(|D\rangle^1 \otimes \Pi_{CC}^{12} |\psi_i\rangle^{12} + |A\rangle^1 \otimes (\mathbb{1} - \Pi_{CC}^{12}) |\psi_i\rangle^{12}) / \sqrt{4}. \quad [9]$$

The approach for Π_{AA}^{12} is similar. In the clockwise path, we place a polarizer and half waveplate to effect the operator $-|D\rangle\langle V|$ and in the other path we place a neutral density filter. The state becomes

$$(|D\rangle^1 \otimes (\mathbb{1} - \Pi_{AA}^{12}) |\psi_i\rangle^{12} + |A\rangle^1 \otimes \Pi_{AA}^{12} |\psi_i\rangle^{12}) / \sqrt{4}. \quad [10]$$

The next step for all three measurements is to project the path state onto $|\psi_f\rangle$ by closing the Pigeon 1 interferometer. A quarter and half waveplate apply a unitary U , which rotates the results of the strong measurement into either the H/V basis, for a real measurement or the R/L basis for an imaginary measurement. The state of Photon 1's polarization at this point is proportional to

$$\langle \psi_f | \Pi |\psi_i\rangle U |D\rangle + \langle \psi_f | (\mathbb{1} - \Pi) |\psi_i\rangle U |A\rangle \quad [11]$$

for any of the three projectors Π .

We use a quantum eraser to erase some, but not all, of the coupling created by the strong measurement. We send the photon into a partial eraser (Fig. 2), which we implement as a displaced Sagnac interferometer that opens and closes with a polarizing beamsplitter. The interferometer couples polarization and path with a strength determined by the angle of two waveplates that enact equal and opposite rotations to photons traveling through either of the two interferometer paths. The strong correlations between polarization and the original pigeon observable are destroyed by projecting the polarization onto an unbiased basis, which incurs another loss factor of 1/2. The path state of the photon just before being detected is proportional to

$$\langle \psi_f | \Pi |\psi_i\rangle |s\rangle + \langle \psi_f | (\mathbb{1} - \Pi) |\psi_i\rangle |-s\rangle, \quad [12]$$

where

$$|s\rangle = \sqrt{\frac{1+s}{2}} |\text{yes}\rangle + \sqrt{\frac{1-s}{2}} |\text{no}\rangle. \quad [13]$$

In a real measurement, $|\text{yes}\rangle$ and $|\text{no}\rangle$ correspond the output ports of the partial eraser. The imaginary measurement rotates these states to the superpositions $(|\text{yes}\rangle \pm i|\text{no}\rangle) / \sqrt{2}$. All told, the variable-strength nonlocal measurement procedure works with probability $1/4$ for Π_S and probability $1/8$ for Π_{CC} or Π_{AA} .

3. Results

The results of our experiment are plotted in Fig. 3. Our goal is to observe properties of the pigeon system, but our data come from measurements of a polarization meter. We call the probability of finding our polarization probe in its real yes state the “real meter value” and the probability for the pigeon system to be in a yes state of our pigeon observable the “real system value.” In a strong measurement, the real meter value is simply equal to the real system value. For weaker measurements, pigeons in a yes state of an observable only shift the meter by a small amount, leaving the meter in the real no state some fraction of the time. To convert meter values to system values, we divide by measurement strength.

Similarly, we call the probability of finding our polarization probe in the imaginary yes state the “imaginary meter value.” To convert to the corresponding “imaginary system value,” we subtract 1/2 (so that a probe in the real yes state registers as having 0 imaginary component) and then divide by measurement strength. In the weak limit, the real and imaginary system values equal the real and imaginary components of the weak value (Eq. 3). In the strong limit, the real system value equals the ABL probability (Eq. 4). The strong limit of the imaginary system value has not been described previously in the literature, but it is related to the sensitivity of the postselection probability to measurement back-action (see Section 4.2 for more details).

All data in Fig. 3 are plotted according to their meter value. Grid slopes represent the conversion between meter values and system values. We begin with the calibration points, which were taken by blocking one path in each pigeon interferometer to postselect the state on one of $|C\rangle|C\rangle$, $|C\rangle|A\rangle$, $|A\rangle|C\rangle$, or $|A\rangle|A\rangle$. These photons should all have a real system value of either 0 or 1 and their real meter values should move toward 1/2 linearly in the measurement strength. Their imaginary meter value should be 1/2 and their imaginary system value should be 0 at all measurement strengths. These predictions (solid lines in Fig. 3) agree qualitatively with our data (points in Fig. 3).

The data postselected on $|+i\rangle|+i\rangle$ are our main results (fuchsia dots in 3). The direct measurements of Π_S (3 a) reveal that the real system value for both pigeons to be in the same hole is indeed consistent with 0 at all measurement strengths. This can be seen from the fact that the real meter value of the $|+i\rangle|+i\rangle$ data is never significantly higher than the $|C\rangle|A\rangle$ or $|A\rangle|C\rangle$ calibration data. While the imaginary values of the $|+i\rangle|+i\rangle$ data do not quite match their predicted value of 0, they are no further from this prediction than the calibration data. Thus, measurement disturbance is not a viable resolution to the quantum pigeonhole paradox.

On the other hand, our data confirm that measurement disturbance does explain the violation of the sum rule. The real part of our $|+i\rangle|+i\rangle$ data is “both clockwise” or “both anticlockwise” significantly more often than it is “both same” at high strengths, but agrees with the “both same” values at weaker strengths. For both strong and weak measurements, the imaginary part of both same significantly differs from the imaginary parts of both clockwise and both anticlockwise. Nevertheless, the sum rule holds because the imaginary parts of both clockwise and both anticlockwise are equal and opposite. While the cancellation of the imaginary parts in the weak limit was predicted by the weak value formula 3, it is remarkable that the cancellation extends into the strong regime, even as the sum rule for the real part fails. The question of whether this kind of cancellation is a general feature of imaginary system values at all measurement strengths is a fascinating avenue for further study.

Fig. 3. Variable-strength measurement results. In each plot, the x -axis denotes measurement strength (Eq. 2) such that 0 is a weak measurement and 1 is a strong measurement. Panels (A–C) show the results for direct measurements of the projectors Π_S^{12} , Π_{CC}^{12} , and Π_{AA}^{12} respectively. The y -axis is the probability for the polarization meter to be in the real yes state. The labeled grid slopes denote the corresponding probability for the pigeons to be in the yes subspace of the projector, after accounting for measurement strength. At small measurement strengths, these values correspond to the real part of the weak value. Each marker and color combination represents a different path postselection. The fuchsia dots represent the paradoxical postselection $|+i\rangle|+i\rangle$. The other four colors are calibration data. Two different theoretical models are plotted for comparison. Solid lines are theory. Dotted lines represent a correction to this theory tomographic calibrations. Panels (D–F) are organized similarly, but their y -axes show the results of measuring in the imaginary basis. At small measurement strengths, the values denoted by the labeled grid slopes correspond to the imaginary part of the weak value. The direct measurements of Π_S^{12} suggest that photons postselected in $|+i\rangle|+i\rangle$ propagate in different directions at least as often as photons which always take the $|C\rangle|A\rangle$ path or the $|A\rangle|C\rangle$ path at all strengths. The disturbance to the meter along its imaginary axis for photons postselected in $|+i\rangle|+i\rangle$ is somewhere between that of $|C\rangle|A\rangle$ path or the $|A\rangle|C\rangle$ for all strengths. Thus, measurement disturbance cannot explain why 3 pigeons among 2 pigeonholes can each be in a different hole. On the other hand, direct measurements of Π_{CC}^{12} and Π_{AA}^{12} show that measurement disturbance is responsible for violation of the sum rule. Strong measurements suggest photons postselected in $|+i\rangle|+i\rangle$ both travel clockwise/anticlockwise a significant fraction of the time, but at weaker measurements, they fall within the no calibration points and agree with the direct measurement of Π_S^{12} .

Having explained the qualitative features of our data, we turn to its quantitative agreement with theory. Most of the discrepancy between our data and theory is accounted for by the quality of our Bell state source and polarization optics. The fidelity of our actual Bell state to the desired one is 95%. Furthermore, the nominally nonpolarizing beamsplitters used to open and close our pigeon interferometers are birefringent, complicating our polarization-based which-path measurements. We measure these effects using polarization state tomography of our Bell state source and polarization process tomography in each path of our pigeon interferometer and use them to generate refined predictions, plotted as dotted lines in Fig. 3. The systematic uncertainty of our data dominates its statistical uncertainty. The error bars in Figs. 3 and 4 denote the RMSD of our calibration data from these refined predictions. They are computed separately for each measurement strength and quadrature (real or imaginary).

To conclude, we realized variable-strength nonlocal measurements to study quantum violations of two seemingly irrefutable counting laws: the pigeonhole principle and the sum rule. Our data show that the violation of the sum rule is an artifact of measurement disturbance. On the other hand, the violation of the pigeonhole principle is the same, regardless of the strength of the back-action. Our experiment shows there is a concrete, empirical, and measurement-independent sense in which three

quantum pigeons really can occupy two holes without any being in the same hole. Finally, our variable-strength apparatus led us to find that the same process that yields the imaginary part of a weak measurement can yield a nontrivial quantity in the strong limit as well. Further exploration of the quantity is a ripe opportunity for further research.

4. Materials and Methods

4.1. Variable-Strength Measurements with a Qubit Meter. The coupling required for a direct measurement of a projector Π on the pigeon system is described by the von Neumann interaction unitary

$$U = e^{-i\theta(2\Pi-1)\otimes\sigma_y} \quad [14]$$

between the pigeon system and a spin-1/2 meter. The meter operator σ_y generates rotations of the initial meter state $|+z\rangle$ by $\pm\theta$ radians in Hilbert space depending on whether the initial pigeon state $|\psi_i\rangle$ is in a yes (eigenvalue 1) or no (eigenvalue 0) eigenspace of Π . Euler's theorem simplifies the unitary to

$$U = \Pi \otimes (\cos \theta \mathbb{1} - i \sin \theta \sigma_y) \quad [15]$$

$$+ (\mathbb{1} - \Pi) \otimes (\cos \theta \mathbb{1} + i \sin \theta \sigma_y). \quad [16]$$

This unitary evolves the initial system and meter state to

$$U|\psi_i\rangle|+z\rangle = \Pi|\psi_i\rangle|s\rangle + (\mathbb{1} - \Pi)|\psi_i\rangle|-s\rangle, \quad [17]$$

Fig. 4. Violation of classical counting principles. The x-axis denotes measurement strength (Eq. 2) such that 0 is a weak measurement and 1 is a strong measurement. The y-axis is the probability for the polarization meter to be in the real yes state. The labeled grid slopes denote the corresponding probability for the pigeons to be in the same hole after accounting for measurement strength. Blue dots show results from direct measurements of the same hole projector Π_S . Orange squares denote an indirect measurement obtained from summing the direct measurements for Π_{CC} and Π_{AA} . Blue and orange slopes denote theoretical predictions for the respective points. The orange region highlights the gap between our two methods for measuring Π_S , indicating a violation of the sum rule. The violation shrinks as the measurement strength decreases. The blue region indicates where direct measurements of Π_S would violate the pigeonhole principle. At all strengths, our direct measurements of Π_S fall in this region.

where

$$|s\rangle = \sqrt{\frac{1+s}{2}}|+x\rangle + \sqrt{\frac{1-s}{2}}|-x\rangle, \quad [18]$$

and $s = \sin \theta$. The meter observable \mathcal{R} for the real basis is calibrated so that

$$\langle \pm s | \mathcal{R} | \pm s \rangle = \frac{1 \pm 1}{2}, \quad [19]$$

which is satisfied when

$$\mathcal{R} = \frac{\mathbb{1} + \sigma_x/s}{2}. \quad [20]$$

The real part of the system value is the expectation of \mathcal{R} conditioned on successful postselection

$$\mathbb{E}[\mathcal{R} | |\psi_f\rangle\langle\psi_f|] = \frac{\mathbb{E}[|\psi_f\rangle\langle\psi_f| \otimes \mathcal{R}]}{\mathbb{E}[|\psi_f\rangle\langle\psi_f|]}, \quad [21]$$

where the expectation value is taken over the coupled state $U|\psi_i\rangle|+z\rangle$. The denominator is the probability that the postselection succeeds.

$$\mathbb{E}[|\psi_f\rangle\langle\psi_f|] = |\langle\psi_f|\Pi|\psi_i\rangle|^2 + |\langle\psi_f|(\mathbb{1} - \Pi)|\psi_i\rangle|^2 \quad [22]$$

$$+ 2\sqrt{1-s^2} \operatorname{Re}[\langle\psi_f|\Pi|\psi_i\rangle\langle\psi_i|(\mathbb{1} - \Pi)|\psi_f\rangle]. \quad [23]$$

The numerator is the joint expectation

$$\mathbb{E}[|\psi_f\rangle\langle\psi_f| \otimes \mathcal{R}] = |\langle\psi_f|\Pi|\psi_i\rangle|^2 + \sqrt{1-s^2} \times \quad [24]$$

$$\operatorname{Re}[\langle\psi_f|\Pi|\psi_i\rangle\langle\psi_i|(\mathbb{1} - \Pi)|\psi_f\rangle]. \quad [25]$$

When $s = 0$, the conditional expectation simplifies to the real part of the weak value (Eq. 3) and when $s = 1$, it simplifies to the Aharonov-Bergmann-Lebowitz formula (34) (Eq. 4).

4.2. Imaginary Measurements. To measure the imaginary part of the weak value, we measure in the imaginary meter basis σ_y . The imaginary meter observable \mathcal{I} is calibrated so that

$$\langle \pm s | \mathcal{I} | \mp s \rangle = \pm i/2, \quad [26]$$

which is satisfied with

$$\mathcal{I} = \frac{\sigma_y}{2s}. \quad [27]$$

The conditional expectation of the imaginary meter observable is

$$\mathbb{E}[\mathcal{I} | |\psi_f\rangle\langle\psi_f|] = \frac{\mathbb{E}[|\psi_f\rangle\langle\psi_f| \otimes \mathcal{I}]}{\mathbb{E}[|\psi_f\rangle\langle\psi_f|]}. \quad [28]$$

The denominator is the postselection probability from the real case treated earlier. The numerator is

$$\mathbb{E}[|\psi_f\rangle\langle\psi_f| \otimes \mathcal{I}] = \operatorname{Im}[\langle\psi_f|\Pi|\psi_i\rangle\langle\psi_i|(\mathbb{1} - \Pi)|\psi_f\rangle]. \quad [29]$$

When $s = 0$, the conditional expectation simplifies to the imaginary part of the weak value (Eq. 3). Curiously, the joint expectation $\mathbb{E}[|\psi_f\rangle\langle\psi_f| \otimes \mathcal{I}]$ does not depend on the measurement strength s at all. If the imaginary part of the weak value is nonzero, the conditional expectation of the imaginary meter observable \mathcal{I} will be nonzero at all measurement strengths. However, this result is specific to a spin-1/2 meter. If the meter was instead the position of a particle, the Euler expansion of the coupling unitary used to evaluate the evolution at all measurement strengths would not be valid.

We have shown how to calculate the conditional expectation of the imaginary meter observable, but we have so far said nothing on how to interpret it. The imaginary part of the weak value is related to the sensitivity of the postselection success probability to the back-action the meter suffers from measuring a system observable (36). The probability P_{ps} of successfully postselecting an initial system state $|\psi_i\rangle$ onto a final system state $|\psi_f\rangle$ is

$$P_{\text{ps}} = \|\langle\psi_f|e^{-i\theta(2\Pi - \mathbb{1}) \otimes \sigma_y}|\psi_i\rangle|+z\rangle\|^2. \quad [30]$$

$$= \langle\psi_i|(+z)e^{i2\theta \operatorname{ad}_{\Pi} \otimes \sigma_y}[|\psi_f\rangle\langle\psi_f|]|\psi_i\rangle|+z\rangle. \quad [31]$$

The super operator ad_{Π} represents the infinitesimal back-action due to measuring Π . The action of ad_{Π} on an arbitrary system operator A is $\operatorname{ad}_{\Pi}[A] = \Pi A - A \Pi$. To describe how the postselection probability changes with the strength of the back-action, we will increase the size of ad_{Π} uniformly with the transformation $i\theta \operatorname{ad}_{\Pi} \rightarrow i\theta \operatorname{ad}_{\Pi} + \delta \mathbb{1} / \sin(\theta)$. δ is an artificial parameter that lets us tune the strength of the back-action independently from

the measurement strength. The postselection probability $P_{ps}(\delta)$ as a function of this back-action parameter is

$$P_{ps}(\delta) = \langle \psi_f | \langle +z | e^{i2\theta \text{ad}_{\Pi} \otimes \sigma_y + 2\delta \mathcal{I}} [|\psi_f\rangle \langle \psi_f | | \psi_i \rangle | +z \rangle \quad [32]$$

$$= \mathbb{E} \left[| \psi_f \rangle \langle \psi_f | \otimes e^{2\delta \mathcal{I}} \right] \quad [33]$$

using the fact that $\mathcal{I} = \sigma_y / (2 \sin \theta)$. The sensitivity of the postselection probability to back-action is

$$\left. \frac{\partial \log P_{ps}}{\partial \delta} \right|_{\delta=0} = 2 \frac{\mathbb{E} [| \psi_f \rangle \langle \psi_f | \otimes \mathcal{I}]}{\mathbb{E} [| \psi_f \rangle \langle \psi_f |]}. \quad [34]$$

The right-hand side of this expression is exactly twice the conditional expectation of the imaginary meter observable.

$$\left. \frac{1}{2} \frac{\partial \log P_{ps}}{\partial \delta} \right|_{\delta=0} = \mathbb{E} [\mathcal{I} | \psi_f \rangle \langle \psi_f |]. \quad [35]$$

In the weak limit, this conditional expectation equals the imaginary part of the weak value. In the strong limit, it may not manifestly be the imaginary part of a complex number, but it is still related to the sensitivity of the postselection probability in the same way.

4.3. Entangled Photon Source. We create photon pairs with a wavelength near 810 nm via type II collinear spontaneous parametric down-conversion. We pump a periodically polled potassium titanyl phosphate (PPKTP) crystal with 2 mW of 405 nm light emitted from a continuous wave laser diode. Before being coupled into a single-mode fiber, each photon passes through a 10 nm band-pass filter centered at 810 nm. The source produces 40,000 pairs per second.

The photons are entangled in polarization because the crystal sits inside a polarizing Sagnac interferometer as shown in Fig. 2. The polarization of the pump is set to $|D\rangle$ so that when pump light hits the two-color (405 nm and 810 nm) polarizing beamsplitter (PBS) that opens the Sagnac, it splits into an equal superposition of illuminating the crystal from the front and back. A two-color half waveplate placed just after the reflected port of the PBS rotates $|V\rangle$ to $|H\rangle$ so that the crystal is illuminated by $|H\rangle$ polarized pump light from both sides. The crystal emits photons in the state $(|HV\rangle|C\rangle + |HV\rangle|A\rangle) / \sqrt{2}$. The photons in the anticlockwise path pass through the two-color half waveplate, rotating their state to $|VH\rangle|A\rangle$. Then the clockwise and anticlockwise paths recombine at the two-color PBS and exit the interferometer with the polarization state $(|HV\rangle + e^{i\phi_S} |VH\rangle) / \sqrt{2}$, where ϕ_S is the relative phase between the two paths in the Sagnac. We apply local polarization rotations on both photons until their state upon exiting the fibers and entering the experiment is as close to $(|HH\rangle + |VV\rangle) / \sqrt{2}$ as possible.

Data, Materials, and Software Availability. Code and data used to reproduce figures and results presented in this manuscript are freely available online at <https://doi.org/10.5683/SP3/DLQU64> (56).

ACKNOWLEDGMENTS. This work was supported by Natural Sciences and Engineering Research Council of Canada and the Fetzer Franklin Fund of the John E. Fetzer Memorial Trust and by Grant No. FQXi-RFP-1819 from the Foundational Questions Institute and Fetzer Franklin Fund, a donor advised fund of Silicon Valley Community Foundation. A.M.S. is a fellow of Canadian Institute for Advanced Research.

Author affiliations: ^aDepartment of Physics and Center for Quantum Information and Quantum Control, University of Toronto, Toronto, ON M5S 1A7, Canada; ^bCanadian Institute for Advanced Research, Toronto, ON M5G 1M1, Canada; and ^cNational Research Council of Canada, Ottawa, ON K1A 0R6, Canada

- A. Einstein, B. Podolsky, N. Rosen, Can quantum-mechanical description of physical reality be considered complete? *Phys. Rev.* **47**, 777–780 (1935).
- D. Frauchiger, R. Renner, Quantum theory cannot consistently describe the use of itself. *Nat. Commun.* **9**, 3711 (2018).
- M. F. Pusey, J. Barrett, T. Rudolph, On the reality of the quantum state. *Nat. Phys.* **8**, 475 (2012).
- L. Hardy, Are quantum states real? *Int. J. Mod. Phys. B* **27**, 1345012 (2013).
- N. D. Mermin, Making better sense of quantum mechanics. *Rep. Prog. Phys.* **82**, 012002 (2018).
- Y. Aharonov, D. Rohrlich, *Quantum Paradoxes: Quantum Theory for the Perplexed* (Wiley-VCH, 2005).
- Y. Aharonov, A. Botero, S. Popescu, B. Reznik, J. Tollaksen, Revisiting Hardy's paradox: Counterfactual statements, real measurements, entanglement and weak values. *Mod. Phys. Lett. A* **301**, 130–138 (2002).
- Y. Aharonov, S. Popescu, D. Rohrlich, P. Skrzypczyk, Quantum Cheshire cats. *New J. Phys.* **15**, 113015 (2013).
- K. Yokota, T. Yamamoto, M. Koashi, N. Imoto, Direct observation of Hardy's paradox by joint weak measurement with an entangled photon pair. *New J. Phys.* **11**, 33011 (2009).
- L. Hardy, Quantum mechanics, local realistic theories, and Lorentz-invariant realistic theories. *Phys. Rev. Lett.* **68**, 2981–2984 (1992).
- A. Brodutch, E. Cohen, A scheme for performing strong and weak sequential measurements of non-commuting observables. *Quant. Stud.: Math. Found.* **4**, 1–15 (2016).
- J. S. Lundeen, A. M. Steinberg, Experimental joint weak measurement on a photon pair as a probe of Hardy's paradox. *Phys. Rev. Lett.* **102**, 20404 (2009).
- M. Leifer, R. Spekkens, Pre- and post-selection paradoxes and contextuality in quantum mechanics. *Phys. Rev. Lett.* **95**, 200405 (2005).
- M. F. Pusey, M. S. Leifer, Logical pre- and post-selection paradoxes are proofs of contextuality. arXiv [Preprint] (2015). <https://arxiv.org/abs/1506.07850> (Accessed 16 October 2019).
- T. Ravon, L. Vaidman, The three-box paradox revisited. *J. Phys. A: Math. Theor.* **40**, 2873–2882 (2007).
- K. J. Resch, J. S. Lundeen, A. M. Steinberg, Experimental realization of the quantum box problem. *Mod. Phys. Lett. A* **324**, 125–131 (2004).
- Y. Aharonov *et al.*, Quantum violation of the pigeonhole principle and the nature of quantum correlations. *Proc. Natl. Acad. Sci. U.S.A.* **113**, 532–535 (2016).
- Y. Aharonov, S. Nussinov, S. Popescu, L. Vaidman, Peculiar features of entangled states with postselection. *Phys. Rev. A* **87**, 014105 (2013).
- A. M. Aredes, P. L. Saldanha, Association between quantum paradoxes based on weak values and a realistic interpretation of quantum measurements. *Phys. Rev. A* **109**, 022238 (2024).
- G. Reznik, S. Bagchi, J. Dressel, L. Vaidman, Footprints of quantum pigeons. *Phys. Rev. Res.* **2**, 023004 (2020).
- M. Waegell *et al.*, Confined contextuality in neutron interferometry: Observing the quantum pigeonhole effect. *Phys. Rev. A* **96**, 052131 (2017).
- M. C. Chen *et al.*, Experimental demonstration of quantum pigeonhole paradox. *Proc. Natl. Acad. Sci. U.S.A.* **116**, 1549–1552 (2019).
- B. E. Y. Svensson, Even quantum pigeons may thrive together. *Proc. Natl. Acad. Sci. U.S.A.* **113**, E3052 (2016).
- Y. Aharonov *et al.*, Reply to Svensson: Quantum violations of the pigeonhole principle. *Proc. Natl. Acad. Sci. U.S.A.* **113**, E3053 (2016).
- R. Corrêa, P. L. Saldanha, Apparent quantum paradoxes as simple interference: Quantum violation of the pigeonhole principle and exchange of properties between quantum particles. *Phys. Rev. A* **104**, 012212 (2021).
- J. P. Groen *et al.*, Partial-measurement backaction and nonclassical weak values in a superconducting circuit. *Phys. Rev. Lett.* **111**, 090506 (2013).
- T. C. White *et al.*, Preserving entanglement during weak measurement demonstrated with a violation of the Bell-Leggett-Garg inequality. *npj Quant. Inf.* **2**, 1–5 (2016).
- M. Hatridge *et al.*, Quantum back-action of an individual variable-strength measurement. *Science* **339**, 178–181 (2013).
- M. Brune *et al.*, Observing the progressive decoherence of the “meter” in a quantum measurement. *Phys. Rev. Lett.* **77**, 4887 (1996).
- N. Katz *et al.*, Coherent state evolution in a superconducting qubit from partial-collapse measurement. *Science* **312**, 1498–1500 (2006).
- G. J. Pryde, J. L. O'Brien, A. G. White, T. C. Ralph, H. M. Wiseman, Measurement of quantum weak values of photon polarization. *Phys. Rev. Lett.* **94**, 220405 (2005).
- D. Lu, A. Brodutch, J. Li, H. Li, R. Laffamme, Experimental realization of post-selected weak measurements on an NMR quantum processor. *New J. Phys.* **16**, 053015 (2014).
- Y. Aharonov, D. Z. Albert, L. Vaidman, How the result of a measurement of a component of the spin of a spin-1/2 particle can turn out to be 100. *Phys. Rev. Lett.* **60**, 1351 (1988).
- Y. Aharonov, P. G. Bergmann, J. L. Lebowitz, Time symmetry in the quantum process of measurement. *Biophys. Rev.* **134**, B1410 (1964).
- F. De Zela, Role of weak values in strong measurements. *Phys. Rev. A* **105**, 042202 (2022).
- J. Dressel, A. N. Jordan, Significance of the imaginary part of the weak value. *Phys. Rev. A* **85**, 012107 (2012).
- A. Hickey, G. Gour, Quantifying the imaginarity of quantum mechanics. *J. Phys. A: Math. Gen.* **51**, 414009 (2018).
- R. Wagner *et al.*, Quantum circuits for measuring weak values, Kirkwood–Dirac quasiprobability distributions, and state spectra. *Quant. Sci. Technol.* **9**, 015030 (2024).
- C. Fernandes, R. Wagner, L. Novo, E. F. Galvão, Unitary-invariant witnesses of quantum imaginarity. *Phys. Rev. Lett.* **133**, 190201 (2024).
- J. Dressel, A. N. Jordan, Weak values are universal in von Neumann measurements. *Phys. Rev. Lett.* **109**, 230402 (2012).
- B. E. Y. Svensson, What is a quantum-mechanical “weak value” the value of? *Found. Phys.* **43**, 1193–1205 (2013).
- B. E. Y. Svensson, On the interpretation of quantum mechanical weak values. *Phys. Scr.* **2014**, 014025 (2014).
- R. Kastner, Weak values and consistent histories in quantum theory. *Stud. Hist. Philos. Sci., Part B* **35**, 57–71 (2004).

44. G. S. Paraoanu, Non-local parity measurements and the quantum pigeonhole effect. *Entropy* **20**, 606 (2018).
45. A. Brodutch, E. Cohen, Nonlocal measurements via quantum erasure. *Phys. Rev. Lett.* **116**, 070404 (2016).
46. K. Resch, A. Steinberg, Extracting joint weak values with local, single-particle measurements. *Phys. Rev. Lett.* **92**, 130402 (2004).
47. A. Brodutch, L. Vaidman, Measurements of non local weak values. *J. Phys.: Conf. Ser.* **174**, 012004 (2009).
48. Z. Q. Wu, H. Cao, H. L. Zhang, S. J. Ma, J. H. Huang, Experimental proposal for performing nonlocal measurement of a product observable. *Opt. Express* **24**, 27331–27339 (2016).
49. Y. Kedem, L. Vaidman, Modular values and weak values of quantum observables. *Phys. Rev. Lett.* **105**, 230401 (2010).
50. K. Edamatsu, Complete and deterministic bell state measurement using nonlocal spin products. arXiv [Preprint] (2016). <https://doi.org/10.48550/arXiv.1612.08578> (Accessed 16 October 2019).
51. K. Yokota, N. Imoto, Linear optics for direct observation of quantum violation of pigeonhole principle by joint weak measurement. arXiv [Preprint] (2018). <https://doi.org/10.48550/arXiv.1812.04887> (Accessed 16 October 2019).
52. X. Y. Xu *et al.*, Measurements of nonlocal variables and demonstration of the failure of the product rule for a pre- and postselected pair of photons. *Phys. Rev. Lett.* **122**, 100405 (2019).
53. Y. Li *et al.*, Experimental nonlocal measurement of a product observable. *Optica* **6**, 1199–1202 (2019).
54. W. W. Pan *et al.*, Photonic realization of erasure-based nonlocal measurements. *Nanophotonics* **8**, 1109–1116 (2019).
55. W. W. Pan *et al.*, Direct measurement of a nonlocal entangled quantum state. *Phys. Rev. Lett.* **123**, 150402 (2019).
56. N. Lupu-Gladstein, Replication Data for: Variable-strength non-local measurements reveal quantum violations of classical counting principles (2024). Borealis. <https://doi.org/10.5683/SP3/DLQU64>. Accessed 6 August 2024.